Eur. Phys. J. B **9**, 659–667 (1999)

THE EUROPEAN PHYSICAL JOURNAL B

EDP Sciences

Log-periodic oscillations for biased diffusion of a polymer chain in a porous medium

V. Yamakov[1,2,a], A. Milchev[1], G.M. Foo[3], R.B. Pandey[2], and D. Stauffer[4]

[1] Institute for Physical Chemistry, Bulgarian Academy of Sciences, G. Bonchev Street, Block 11, 1113 Sofia, Bulgaria
[2] Department of Physics and Astronomy, University of Southern Mississippi, Hattiesburg, MS 39406-5046, USA
[3] Supercomputing and Visualization Unit, National University of Singapore, Singapore, 119620
[4] Institute for Theoretical Physics, Cologne University, 50923 Köln, Germany

Received 7 August 1998

Abstract. A coarse-grained off-lattice bead-spring model is used to reveal the complex dynamics of a polymer chain in a quenched porous medium in the presence of an external field B. The behavior of the mean square displacement (MSD) of the center chain bead and that of the center of mass of the chain as a function of time is studied at different values of the barrier concentration C, the field strength B and the chain length N. In a field, important information on the way in which chains move between obstacles and overcome them is gained from the MSD *vs.* time analysis in the directions parallel and perpendicular to the flow. Instead of a steady approach to uniform drift-like motion at low C, for sufficiently strong field B we observe *logarithmic oscillations* in the effective exponents describing the time dependence of the MSD along and perpendicular to field. A common nature of this phenomenon with oscillatory behavior, observed earlier for biased diffusion of tracers on random lattices, is suggested.

PACS. 36.20.-r Macromolecules and polymer molecules – 82.45.+z Electrochemistry and electrophoresis – 87.15.-v Biomolecules: structure and physical properties

1 Introduction

The transport behavior of a polymer chain is generally studied by analyzing the time dependence of the mean square displacement (MSD) of a monomer of a chain (g_1) and that of the center of mass of the chain molecule (g_3) which are defined by

$$g_1(t) = \langle [r_{N/2}(t) - r_{N/2}(0)]^2 \rangle$$
$$g_3(t) = \langle [r_{CM}(t) - r_{CM}(0)]^2 \rangle, \quad (1)$$

where $r_{N/2}(t)$ ($r_{CM}(t)$) is the position of the center node (center of mass of the chain) at time t. A common practice in such analysis is to look for the leading power-law dependence of these mean square displacements described by the exponents ν_1 and ν_3,

$$g_1(t) \sim t^{\nu_1}$$
$$g_3(t) \sim t^{\nu_3}. \quad (2)$$

For Fickian diffusion, the value of the power-law exponent is 1. The dynamics of polymer chains has been extensively studied in melts where the motion of each chain is hindered by the presence of surrounding chains causing "entanglements". In an ideal chain model of a melt, the mean square displacements exhibit various power laws in different time regimes [1–3]. The magnitude of these power-law exponents is well known from the short to the long time regimes, *i.e.*, for a monomer (bead/node) motion, $\nu_1 = 1$ (diffusion), 1/2 (Rouse), 1/4 (constrained Rouse), 1/2 (reptation), and 1 (diffusion) finally in the asymptotic limit while the corresponding exponents for the center of mass, $\nu_3 = 1$, 1/2, and 1 spanning over the whole time regime. For single molecules instead of chains, diffusion in a fixed bias was discussed since many years [4–8].

We have recently studied the dynamics of a polymer chain in a quenched random medium using a Monte Carlo simulation [9,10]. We used an off-lattice bead-spring model of a polymer chain in three dimensions with a random distribution of quenched obstacles. We found that the power-law dependence of the mean square displacements in the short time regime is modified from that of an ideal melt mentioned above: the MSD exponents ν_1 and ν_3 depend on the obstacles/barriers concentration [9].

We would like to extend this study to the motion of a polymer chain in a quenched porous medium in the presence of a constant field. In absence of quenched barriers (porosity 1), the field drives the chain to drift and one would expect a crossover from a diffusive behavior at short time scales to a drift-like motion in the long time regime. The problem becomes more complex due to the presence of quenched barriers as one begins to increase the barrier

[a] e-mail: yamakov@ipc.bas.bg

concentration (*i.e.* reduce the porosity). One may expect not only the crossover behavior to change but the exponents for the power-law dependence may be altered as the field begins to compete with the barriers.

Earlier [11] we have carried out an off-lattice computer simulation study of the motion of a bead-spring chain for different chain lengths (*i.e.* number of beads) N in a porous matrix with random distribution of quenched barriers, investigating the impact of bias and obstacle concentration on drift velocity and the conformational properties of the polymer chains. Related work on the motion of particles by ac forces in periodic structures [12], electrophoresis of polyelectrolytes [13,14] and gel electrophoresis for polymers with impurities [15] has provided valuable theoretical insight into this field although computer experiments could shed more light into intricate details of the problem. Effects of bias, barrier concentration (porosity), polymer concentration, and temperature on the conformational and transport properties of chains have been extensively studied using discrete lattice models in recent years [16–19].

In the present work we focus on the behavior of the effective exponents for a wide range of B and C values, where B denotes the external field and C is the barrier concentration, using an off-lattice model with a bead-spring chain. While we recover the standard dynamics of the chain for extreme values of the parameters, *i.e.*, $B \to 0$, $C \to 0$, we observe unusual transport behavior in certain concentration regimes ($C \sim 0.75$) in relatively high field. For example, the power-law behavior of the MSD exhibits logarithmic oscillations in ν_1 and ν_3. In this respect a rather complex system, such as a polymer chain driven through a random medium, reveals close resemblance to the oscillatory behavior of MSD exponents, found for tracer atoms in biased diffusion on percolative lattices, predicted theoretically [4], and observed in simulations [6,7]. On a lattice with strong bias, walkers are trapped for a time growing exponentially with the length of the trap in bias direction; since they need one, two, three ... backward steps to escape, the logarithm of the trapping times increases by constant intervals, leading to the log-periodic oscillation. In our off-lattice model, the discrete structure is less pronounced, leading to weaker oscillations in agreement with our observations. As in the case of random walkers on a simple cubic lattice in the presence of an electric field [6], also for chains we find that the period of such logarithmic oscillations, λ, grows with increasing average distance between obstacles. Our findings are also consistent with the simulational results of Stauffer and Sornette [7], who observe an increase of λ as the field strength B is increased. The model is described in the next section, followed by results and discussion with a summary at the end.

2 The model

We use an off-lattice bead-spring model [20] for the polymer chain in a three-dimensional porous medium generated by a random distribution of quenched obstacles/barriers. Since details of the model have been given before [20], in the following we only recall the potentials involved in the chain model, define the porous medium, and the physical quantities measured.

2.1 The coarse-grained polymer chain

The bead-spring model has been used extensively in the past [10,21–26]. A coarse-grained polymer chain of length N consists of N beads/monomers which are successively connected by spring bonds using a finitely extensible nonlinear elastic (FENE) potential,

$$U_{\rm FENE} = -\frac{K}{2}R^2 \ln[1 - (\frac{l - l_0}{R})^2] \qquad (3)$$

where l is the bond length, $R = l_{\rm max} - l_0$, while l_0, $l_{\rm max}$, and $l_{\rm min}$ are the equilibrium value of the effective bond length, and its maximum and minimum values, respectively, such that $l_{\rm min} < l < l_{\rm max}$ and $l_{\rm min} = 2l_0 - l_{\rm max}$. As in most studies using this model, we set $l_{\rm max} = 1$, $l_{\rm min} = 0.4$, $l_0 = 0.7$. The associated spring constant K is fixed at $K = 40$, where the energy units are defined by setting the parameter ϵ (see below) to unity.

The non-bonded interactions among the beads are described by the Morse potential,

$$U_{\rm M}(r) = \epsilon[\exp(-2\alpha(r - r_{\rm min})) - 2\exp(-\alpha(r - r_{\rm min}))] \qquad (4)$$

where r is the distance between the centers of the beads and at $r_{\rm min} = 0.8$ the potential (4) has its minimum: $\epsilon = 1$. The parameter $\alpha = 24$ is chosen here such that the interaction is negligible at distances larger than unity. These values of the parameters of the potentials are used to implement an efficient *link-cell* algorithm which takes into account the short range interactions. With this choice of parameters of the potentials, equations (3, 4), the radius of the bead is large enough to ensure that chains do not intersect.

2.2 The external field

An external field or bias, B, is implemented *via* a change in energy $-B\delta x$ involved with each movement of a monomer by δx along the field ($x-$) direction. The magnitude of the step length δx is selected randomly between 0 and a fixed small value ($\delta x_{\rm max} = \pm 0.5$ here). The Metropolis algorithm is used to move a randomly selected bead in a randomly selected direction with randomly selected step length δx, δy, and δz with probability $\min\{1, \exp[-(E_{\rm new} - B\delta x - E_{\rm old})/k_{\rm B}T]\}$, where $E_{\rm old}$ and $E_{\rm new}$ are energies (FENE and Morse) in the old and new configurations, respectively. An attempt to move each bead once is defined as a unit Monte Carlo step (MCS) of time.

2.3 The porous medium

The porous medium is generated by a random distribution of quenched immobile particles each of which interacts with the beads *via* the Morse potential equation (4). The choice of the minimum of the potential at $r_{\min} = 0.8$ from the center gives an estimate of the diameter of the spherical Morse particle. The hard core volume of a pore barrier particle is therefore, $v_{\rm p} = \frac{4}{3}\pi(\frac{r_{\min}}{2})^3 \simeq 0.268$. The barrier concentration C is defined as the number of particles per unit cell which may also be referred to as a number density. Thus, as long as the volume of a particle is less than 1, a number density or concentration $C > 1$ is allowed. An effective percolation threshold of the porous medium is achieved at the barrier concentration $C \simeq 1.1$ [27]. In order to have well connected (spanning) pores, the pore volume space must be above the pore-percolation threshold, *i.e.*, the barrier concentration must be below $C = 1.1$. In a field, the movement of chains becomes too slow to draw meaningful conclusions closer to the threshold. In this study, the concentration of the obstacles C is varied between 0 and 0.875, well below the threshold.

The temperature is kept constant at $k_{\rm B}T = 2.0$ so as to simulate the good solvent condition since from previous studies of the model [21] the $\theta-$temperature is known to be $k_{\rm B}T_\theta = 0.62$ in absence of the field. In this way we make sure that the short-ranged attractive Morse interactions between the beads will be considerably below the bead's thermal energy and will have little effect on the interaction of the drifting chains with the frozen obstacles.

2.4 Physical quantities

The behavior of the mean square displacements (MSD) of the chain's central bead (g_1) and of its center of mass (g_3), defined by equation (1), is studied in detail along with the radius of gyration as a function of the barrier concentration and field strength. During the simulation, we also keep track of mean bond length and energy.

Since the external field introduces a preferred direction for the motion of the chain nodes, we analyze the longitudinal and transversal components of the MSD separately, *i.e.*, the longitudinal displacements

$$\begin{aligned} g_{1\rm L}(t) &= \langle [x_{N/2}(t) - x_{N/2}(0)]^2 \rangle \\ g_{3\rm L}(t) &= \langle [x_{CM}(t) - x_{CM}(0)]^2 \rangle, \end{aligned} \tag{5}$$

along the bias field direction, and the transversal displacements,

$$\begin{aligned} g_{1\rm T}(t) &= \langle [y_{N/2}(t) - y_{N/2}(0)]^2 + [z_{N/2}(t) - z_{N/2}(0)]^2 \rangle, \\ g_{3\rm T}(t) &= \langle [y_{CM}(t) - y_{CM}(0)]^2 + [z_{CM}(t) - z_{CM}(0)]^2 \rangle. \end{aligned} \tag{6}$$

perpendicular to the bias field.

The power-law exponents $\nu_{1\rm L}, \nu_{1\rm T}$, defined by equation (2), are determined from the slope of the $\ln(g_{1\rm L/T})$ *vs.* $\ln(t)$ curve at time t,

$$\nu_{1\rm L/T}(t) = {\rm d}\ln[g_{1\rm L/T}(t)]/{\rm d}\ln(t) \tag{7}$$

which, in a discrete form, can be written as,

$$\begin{aligned} &\nu_{1\rm L/T}[(t_n + t_{n-1})/2] \\ &\qquad = \ln[g_{1\rm L/T}(t_n)/g_{1\rm L/T}(t_{n-1})]/\ln(t_n/t_{n-1}) \end{aligned} \tag{8}$$

where t_{n-1} and t_n are two consecutively measured times. Similar expressions are used to evaluate $\nu_{3\rm L}$ and $\nu_{3\rm T}$ from the corresponding displacements $g_{3\rm L}$ and $g_{3\rm T}$.

2.5 Simulation parameters and statistics

The simulations are performed in a volume of 64^3 cells with obstacle concentrations ranging from $C = 0$ to $C = 0.875$ (229376 bead particles) to form the porous medium. The length of the diffusing chain, immersed into this host matrix, assumes the values $N = 1, 4, 8, 16, 32, 64$ and 128 monomers. The intensity of the external field B is varied from 0.125 to 2.0 relative units (in our case *energy* in $[k_{\rm B}T]$ per *distance* in unit lengths), so that the average potential energy, gained by the particle due to the field in 1 MCS is much less than the kinetic or heat energy per particle (note that the average absolute value of randomly generated displacements is $|\Delta x| = 0.25$ which coupled with $B \leq 2.0$ gives more than four times smaller energies than the heat energy $k_{\rm B}T = 2.0$ used in the simulations). To obtain better statistics all the measurements have been averaged over 20 to 50 independent random media. Since the required computational effort is considerable, typically the length of the runs was set to 10^6 MCS.

Another way to improve the statistics of our measurements, used in the present study, is to move many non-interacting (interpenetrable) chains (each driven polymer in the system does not "feel" the other driven polymers and can penetrate through them), and to average observations over all chains. It should be clear that our results apply strictly to the case of very dilute polymer solutions when polymer coils do not interact with each other and, therefore, do not jam or block narrow channels or "bottlenecks" in the host matrix for each other.

3 Results and discussion

3.1 Power-law variation of MSD

The time dependence of the mean square displacements of the center of mass of the chain and that of its center node (g_3 and g_1) is studied in detail as a function of field (B) and barrier concentration (C) for different chain lengths. As mentioned above, the field is applied in $x-$direction, therefore, the displacements along the longitudinal (x) and transversal (y, z) directions may be different, *i.e.* an anisotropy in the displacement is expected due to the field. The displacements may further be modified by the presence of quenched barriers. Therefore, the longitudinal and transversal components of the displacements are analyzed separately to see the changes in their variations directly. Further, as in most studies, we look

for the power-law dependence of the MSDs described by equation (1).

In an ideal system, *i.e.*, for the motion of a particle executing its stochastic motion in a biased field, one would expect a power-law dependence of the ms displacement, $g \simeq At^{k_1} + Bt^{k_2}$, where the exponents k_1 and k_2 describe the diffusive and drift behavior with their ideal values 1 and 2, respectively. The crossover from diffusion to drift in time as a function of bias in the variations of the mean square displacement and corresponding exponents are relatively well understood. The motion of such diffusing particles under bias in the presence of quenched barriers (*i.e.* in a porous medium) becomes very complex as the bias begins to compete with the barriers. However, one usually studies the MSDs using a leading power-law described by a single exponent, equation (1), and examines the variation of the exponent with field and barrier concentration.

In the present work we examine our data for the MSD of the center node of the chain and that of its center of mass using such a power-law. A typical variation of the longitudinal and transversal MSD's with time is presented in Figure 1a. It is interesting to note that at comparatively short times (10^2–10^3 MCS) larger MSDs are observed perpendicular to the bias whereas for large time intervals ($> 10^4$ MCS) the overall movement along the field prevails. The slope of these data provides an estimate of the effective exponent. A crossover between the short time behavior with a smaller slope and the long time behavior with a larger slope is evident for both longitudinal and transversal components. Further, the MSD of the center of mass merges with that of the center node at times when the chain starts moving along the field as a whole (at $\approx 10^5$ MCS), while for a further decay of time the transversal MSD of the center monomer overtakes the transversal movement of the center of mass. Thus clearly the motion of a chain node is more complex than that of a free particle as mentioned above. For ν_1 and ν_3 the onset of oscillations periodic in the logarithm of time [8] is demonstrated in Figure 1b where in a time interval of 10^7 MCS more than three modulations are seen.

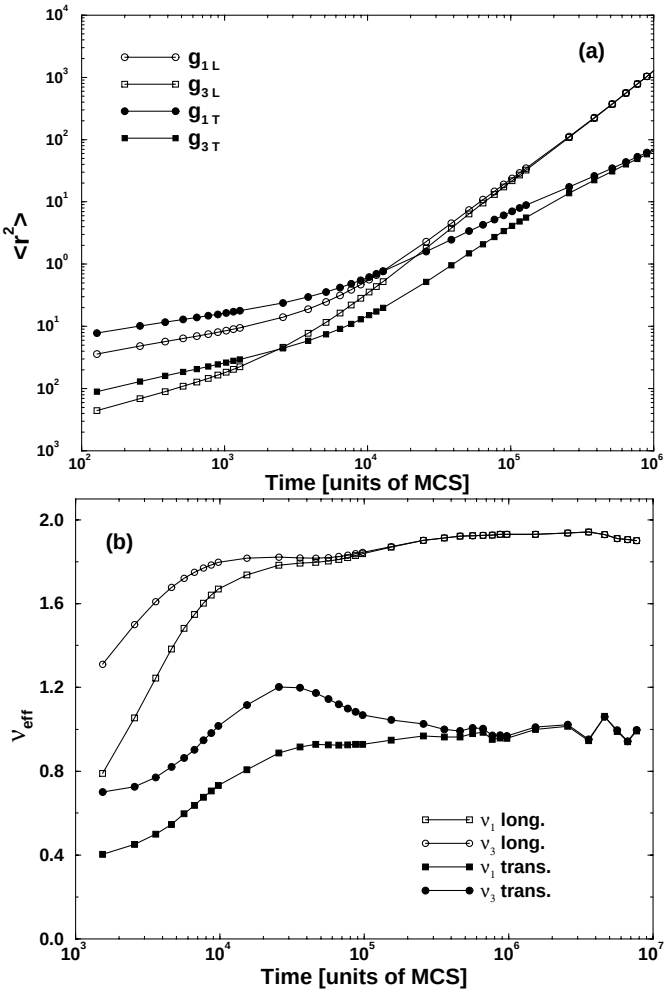

Fig. 1. (a) Mean square displacement *versus* time of a chain of 32 beads in a box of 64^3 cell size with periodic boundary conditions. The intensity of the biasing field is $B = 1.5$ in k_BT units and the obstacle concentration is $C = 0.75$. The data was averaged over 100 runs of 16 chains each in about 50 independent porous media. (b) Log-oscillations in ν_1 and ν_3 for chain length $N = 32$ and $C = 0.50, B = 0.375$

In order to study the change in the power-law behavior more closely, we evaluate the exponent periodically in small time intervals and examine the variation of its magnitude with time. The variation of the corresponding exponents for the longitudinal components of the MSD with time is presented in Figure 2 at various values of field with different chain lengths at the barrier concentration $C = 0.50$. Since results with reasonable statistics require considerable computational efforts, our simulations span a time interval of 10^6 MCS whereby only the first modulation of $\nu_{\rm eff}$ is clearly observed. The longitudinal exponent ($\nu_{\rm effL}$) for a single particle (chain length one) shows a nice crossover from a diffusive behavior ($\nu_{\rm effL} \sim 1$) in the short-time regime to a drift behavior ($\nu_{\rm effL} \sim 2$) in the long-time regime. We note that the crossover time depends on the magnitude of the field (B): the smaller the field, the longer it takes to reach the drift motion. On increasing the chain length ($N = 4, 8, 16$), we see a trend for such a crossover to take longer. In addition, the magnitude of the exponent seems to decay somewhat with time, also the short time value of the exponent for the center node of the chain (ν_1) is smaller than that for the center of mass as expected.

On increasing the chain length further to $N = 32$ and 64, logarithmic oscillations begin to develop in the variation of the long time values of the exponent. Further we note that the larger the chain, the larger is the oscillation's period and amplitude. For the long chain ($N = 64$), the exponent shows a maximum which becomes more pronounced at higher values of the field.

The variation of the longitudinal exponent ν_{3L} in terms of the average distance r traveled by the chain center of mass from the beginning of the measurement is plotted in Figure 3. Evidently, the distance when ν_{3L} reaches its first maximum grows steadily with decreasing intensity of the field B, that is, the transition from diffusive to drift motion takes place faster with larger values of the bias – Figure 3a. The value of the maximum itself is considerably lower for

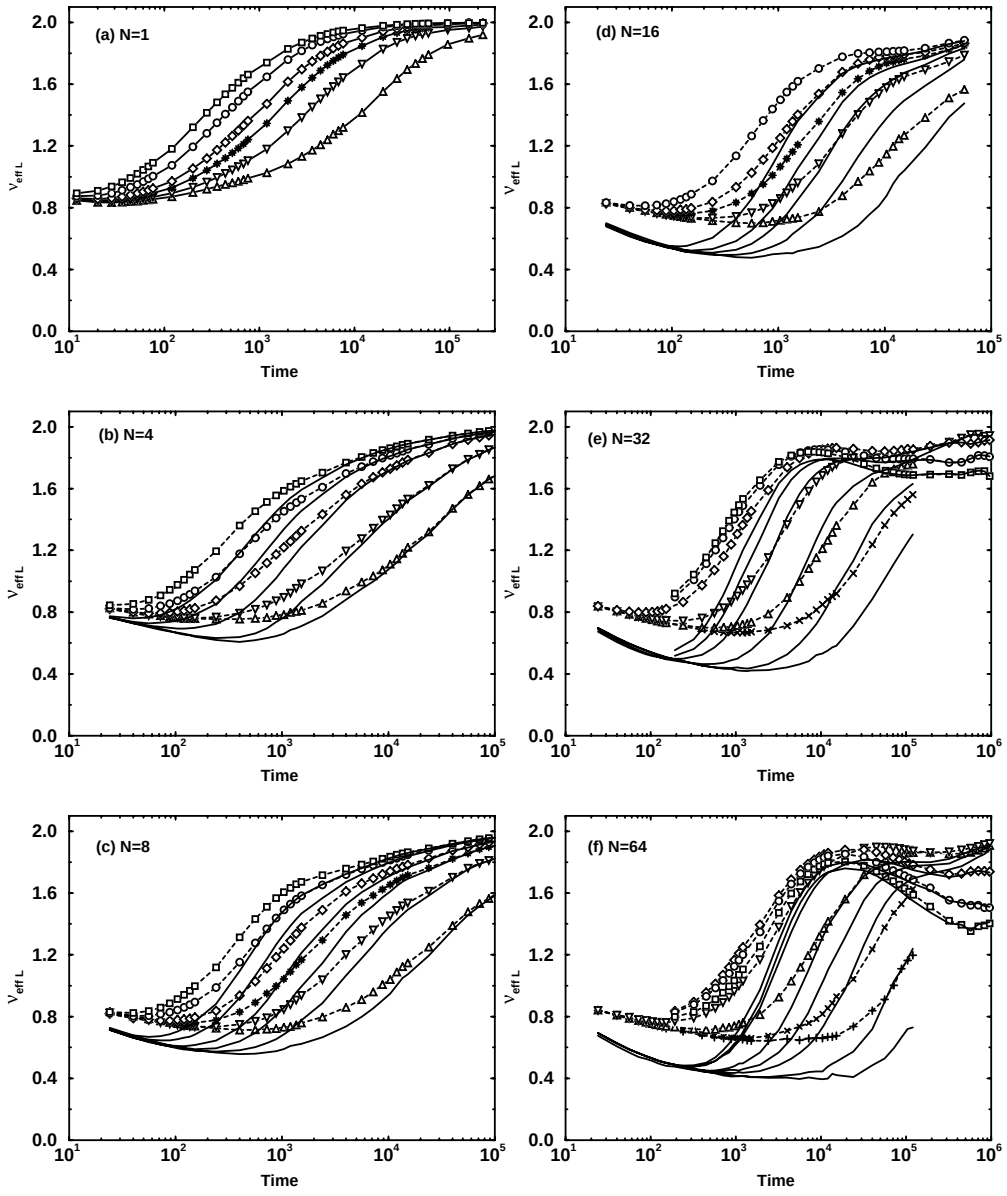

Fig. 2. Longitudinal effective exponent *vs.* time at $C = 0.50$, for various bias fields and chain lengths as marked in the figure. The symbols correspond to a bias field B as follows: (+) 0.0625, ($\times$) 0.125, ($\triangle$) 0.25, ($\bigtriangledown$) 0.50, ($*$) 0.75, ($\diamond$) 1.0, ($\bigcirc$) 1.5 and ($\square$) 2.0. The symbols connected by dashed lines give the center of mass exponent while the solid lines give the corresponding exponent of the center bead of the chain. Time is given in MCS-units everywhere.

very strong biases ($B > 5$) when polymer chains spend most of their time hooked at obstacles and the monomers can hardly perform transversal moves so as to disentangle and subsequently drift with the field. Within the total length of the measurement (10^6 MCS), the MSD of chains at such intensity of the field is about 40 times smaller than the distance reached at moderate bias strength $1 < B < 5$. For $B < 1$ the field is already too weak to carry the chain sufficiently far. Despite such difficulties of the measurement the first period of log-oscillations is clearly seen in Figure 3a, moreover, the period of the oscillation λ visibly grows with growing bias as the careful analysis of Figure 3a shows. It is remarkable that this finding for a rather complex system of bead-spring chains protruding into the frozen matrix of randomly distributed obstacles agrees very well with the simulational results for the much simpler case of biased diffusion which tracer atoms may perform on random lattices [6,7].

In Figure 3b we show the progressive shortening of λ, the oscillation period, with increasing concentration of the obstacles C (for $C = 0$ the chain's drift is unperturbed and no oscillations exist). Evidently, the period λ

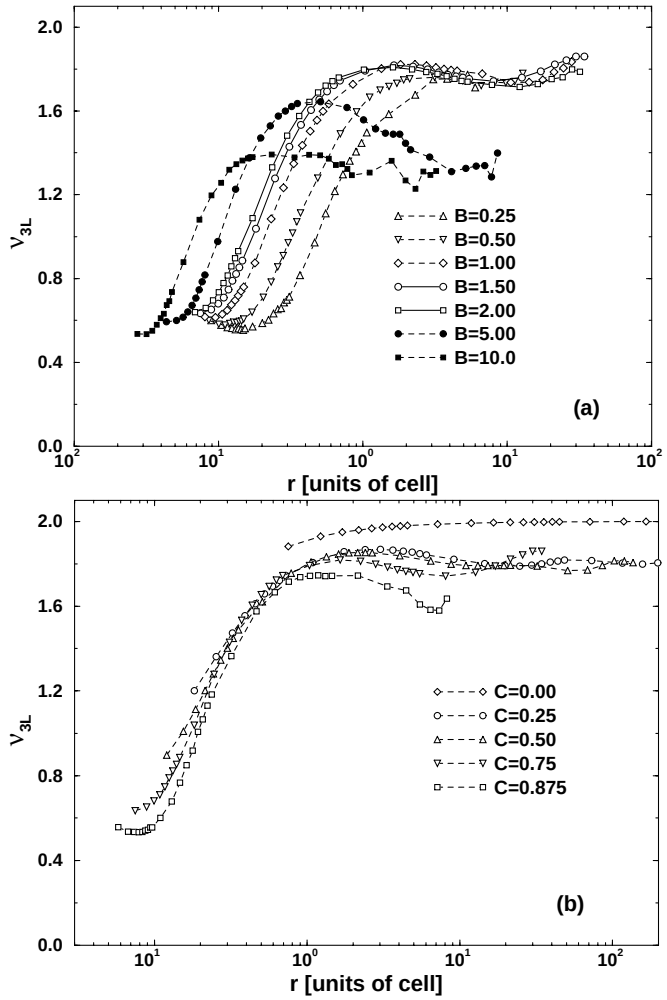

Fig. 3. ν_{3L} *vs.* displacement from the starting point r for: (a) various bias fields at $C = 0.75$, and (b) for various obstacle concentrations at $B = 1.5$. The chain length in both cases is $N = 32$.

is related to the changing average distance between barriers in the medium. The simulations of random walkers [6] find a similar decrease of λ with increasing concentration of the blocking sites.

A signal of the oscillatory behavior in the effective power-law exponent with overshoot and undershoot is also observed for the transversal component of the MSD (see Fig. 4). As for the exponent ν_{3T}, log-oscillatory behavior appears for weaker fields B and at smaller chain lengths N than for ν_{3L}. A distinct difference between the instantaneous values of the exponents for the transversal component of the MSD of the center node and that of the center of mass arises quickly for longer polymer chains, $N > 8$. The amplitude of the log-oscillations is much more pronounced for the center of mass exponent than for the middle monomer, suggesting a trend toward nearly drifting transversal motion for the chain as a whole with increasing chain length ($\nu_{\mathrm{effT}} \approx 1.6$) at time ($\sim 10^4$ MCS) where the first maximum occurs. In the same time regime the middle monomer already performs a purely diffusive motion ($\nu_{\mathrm{effT}} \approx 1$) perpendicular to the field. Intuitively this can be attributed to the circumventive motion of the chain around an obstacle. Comparison with Figure 3a shows that the oscillations in the transversal exponent ν_{effT} take place simultaneously with those of ν_{3L}, suggesting that the transversal displacement is not independent of the longitudinal movement of the chain, as demonstrated in Figure 5.

The position of $t_{\max}$, the first maximum of ν_{3T} in time, can be easily determined – the plot shown in Figure 5f yields $t_{\max} \propto N$. In contrast, for the chain lengths used in this study, we find that the spatial position of this maximum, *i.e.* the mean-square displacement perpendicular to the field, is nearly constant or decreases rather slowly with N. Thus Figure 5f appears consistent with the N^{-1} dependence of the diffusion coefficient on chain length typical for the Rouse-like polymer dynamics of our model. Indeed, in the direction perpendicular to the field B, one would expect the motion of the driven chain to be purely diffusive. The typical time $t_{\max}$, needed by the chain to travel the certain distance which corresponds to the first oscillation maximum, should be inversely proportional to the chain's diffusion coefficient D, and, therefore, for Rouse diffusion $t_{\max}$ should grow linearly with the chain length N.

3.2 Variation of gyration radius with barrier concentration and field

In this section we report some simulational results concerning the average size of the polymer chains which are driven by the field through the random host matrix. These findings supplement the rather complex picture of biased diffusion, observed in the present study, demonstrating that the size of the penetrating objects is strongly dependent on the porosity of the medium and the intensity of the applied external field [18,28].

Figure 6 shows plots for the scaled MS gyration radius (R_{g}) with barrier concentration and field. First, we note that R_{g} depends nonmonotonically on the barrier concentration (Fig. 6a). Introducing quenched barriers (*i.e.* increasing C from zero), seems to elongate the chain as they are forced to explore the narrowing cavities in the host matrix. For the short chains, $N = 16$, this effect is missing because they still fit into the free volume between the obstacles. For $N = 32$, and especially for $N = 64$, with growing density of barriers the elongation/spreading in the low concentration regime increases. On further increasing the barrier concentration these chains begin to be confined by the walls of the pores instead, resulting in a lower R_{g}. Thus there is a characteristic concentration at which the gyration radius is maximum. More thoroughly this relationship has been investigated in our previous works [11,16].

The response of the gyration radius to changing intensity of the field also exhibits a nonmonotonic behavior – Figure 6b. At $C = 0.75$, R_{g} increases on increasing the field B until a characteristic value (B_{c}) is reached beyond which it begins to decline. In low field regimes, the chains continue to elongate on increasing field until they begin to get hooked at the barriers. The larger the chain length is,

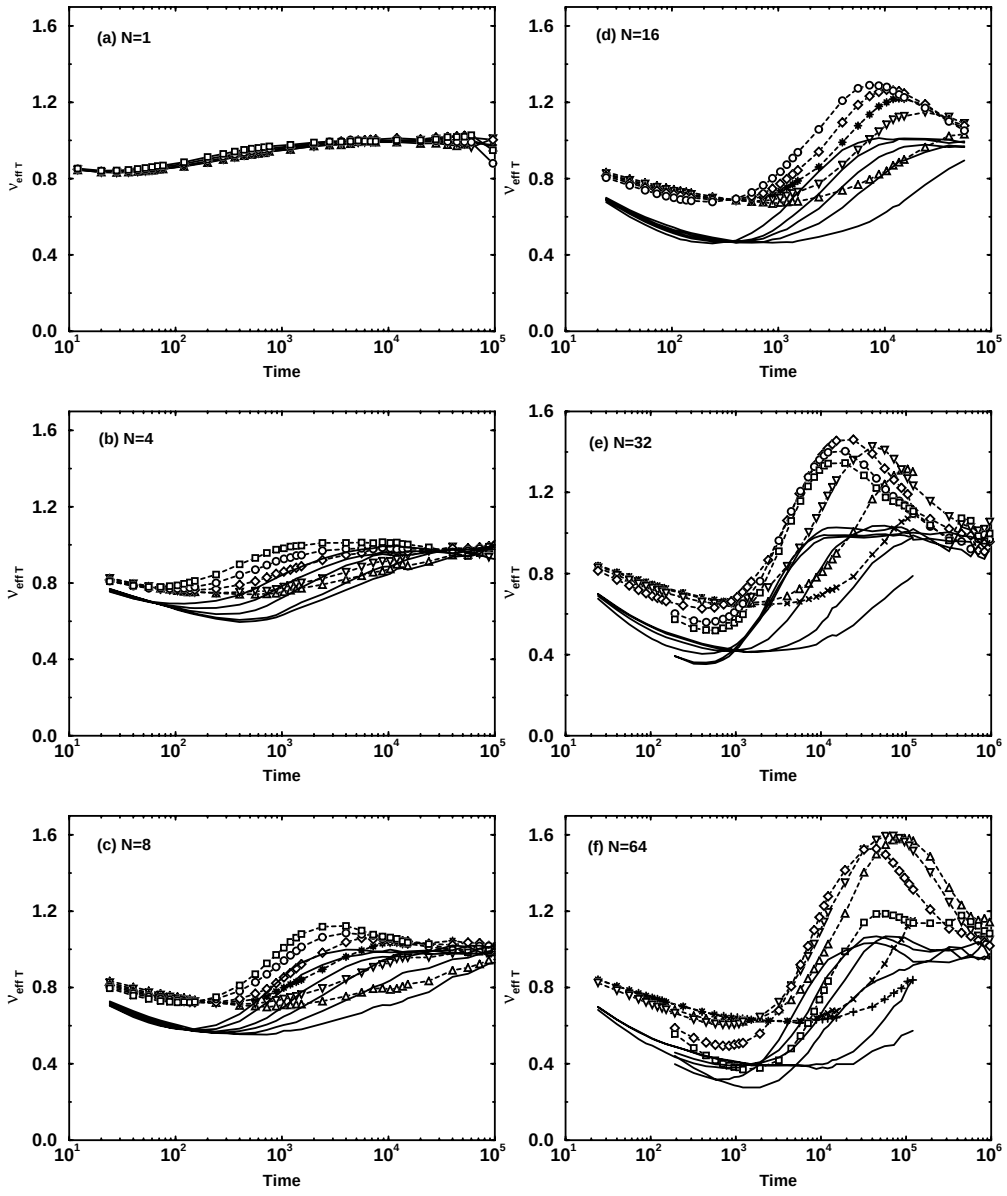

Fig. 4. Transversal effective exponent *vs.* time t at $C = 0.50$, for various bias fields and chain lengths as marked in the figure. The legend is the same as in Figure 2. Time is given in MCS-units everywhere.

the higher is the probability of such an encounter. Therefore, the characteristic field (B_{c}) increases on decreasing the chain length. We are unable to provide here a more quantitative nature of such a decay, due to the limited set of data points; however, a power-law decay of such a characteristic field with the chain length has been observed in a somewhat different system dealing with a lattice model [16].

Similar to the R_{g}^2 *vs.* B relationship, a nonmonotonic dependence, characterized by a "critical" intensity B_{c}, is also observed in the drift velocity (see Fig. 7). Recently [11] we found that $NB_{\mathrm{c}} \approx$ const. Again we would like to point out a close resemblance with some earlier results [5,29,30] on the influence of an electric field on random walkers in a random environment. While in reference [30] it has been predicted that for a certain bias the drift velocity will vanish, our rather complex moving objects follow rather the prediction [5,29] (for tracer atoms under strong influence of the electric field) that for high bias the drift will be reached after long times.

Thus, the competition between field strength and barrier concentration leads to a nonmonotonic behavior of the conformational properties, and to a nonlinear response which is beyond the description in the framework of traditional linear response theories.

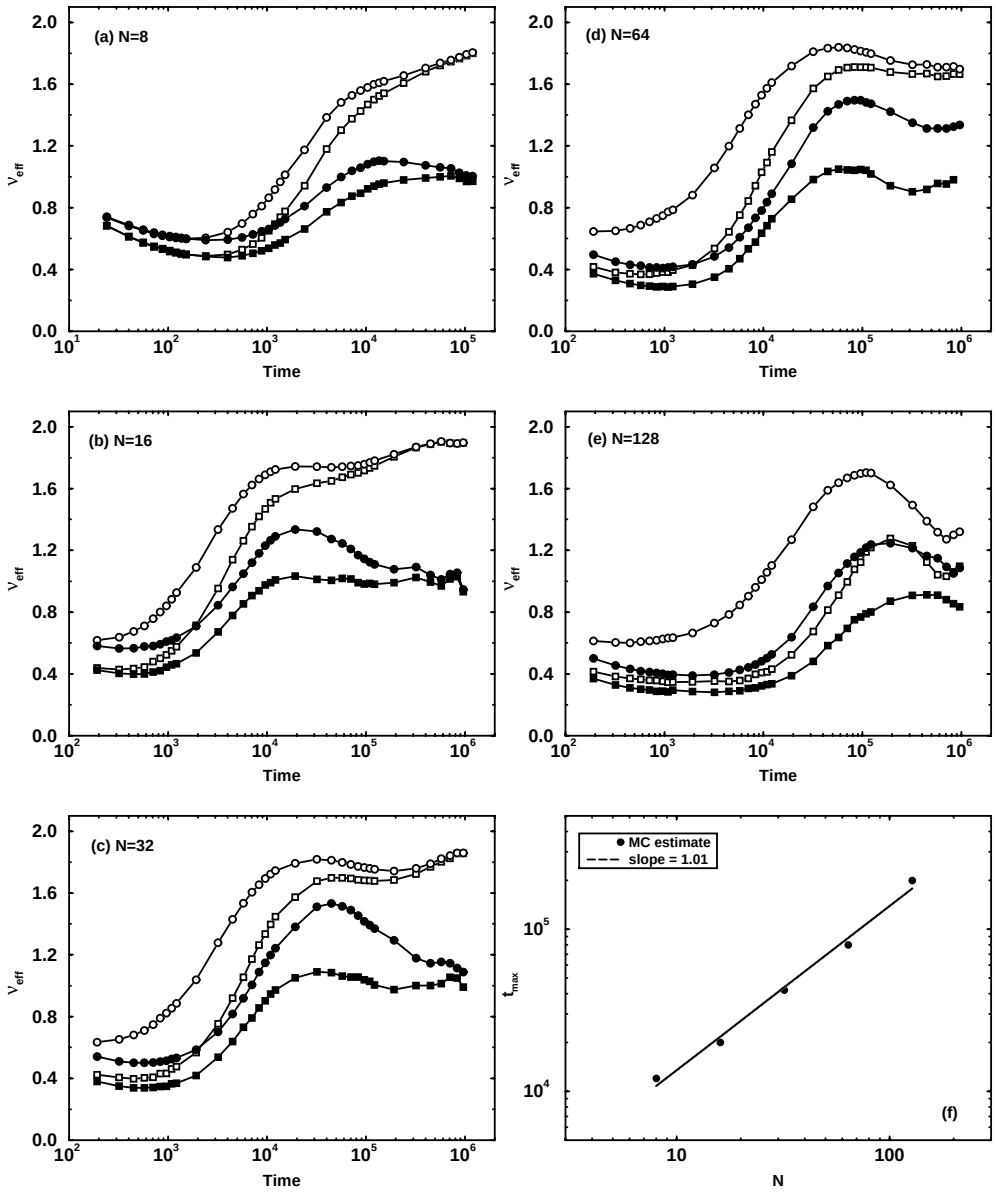

Fig. 5. (a)-(e) Longitudinal (empty symbols) and transversal (full symbols) effective exponent *vs.* time t at $C = 0.75$ and $B = 1.5$ for various chain lengths as marked on the figures. The circles (◯) correspond to the center of mass effective exponent, while the squares (□) correspond to the effective exponent of the center bead of the chain. (f) The first maximum of the center of mass transversal effective exponent in time $t_{\max}$ *vs.* chain length N. Time is given in MCS-units everywhere.

4 Summary

We use an off-lattice bead-spring model of a coarse-grained polymer chain to study polymer chain dynamics in a host matrix of randomly distributed obstacles under the influence of an external field. Our main concern is the behavior of the exponent describing the MSD/time variation. We find that the presence of a sufficiently strong field and the interaction between the chain and the obstacles leads to logarithmic oscillations of the exponents describing the chain's movement along and perpendicular to the field direction.

As in some earlier studies of tracer atoms, performing biased diffusion on a random lattice, we find that the oscillation period of the exponent modulation increases as the bias and the mean "free path" of the chains in the host matrix are increased. Clearly, some questions concerning, for instance, the total number of oscillations of $\nu_{\rm eff}$, or their rate of decay with elapsed time, remain unanswered by the present study. A more quantitative investigation would require larger systems and much more computing time. However this is left for future work.

Finally, it is hoped that our work will stimulate interest to study biased diffusion of polymer chains in a random

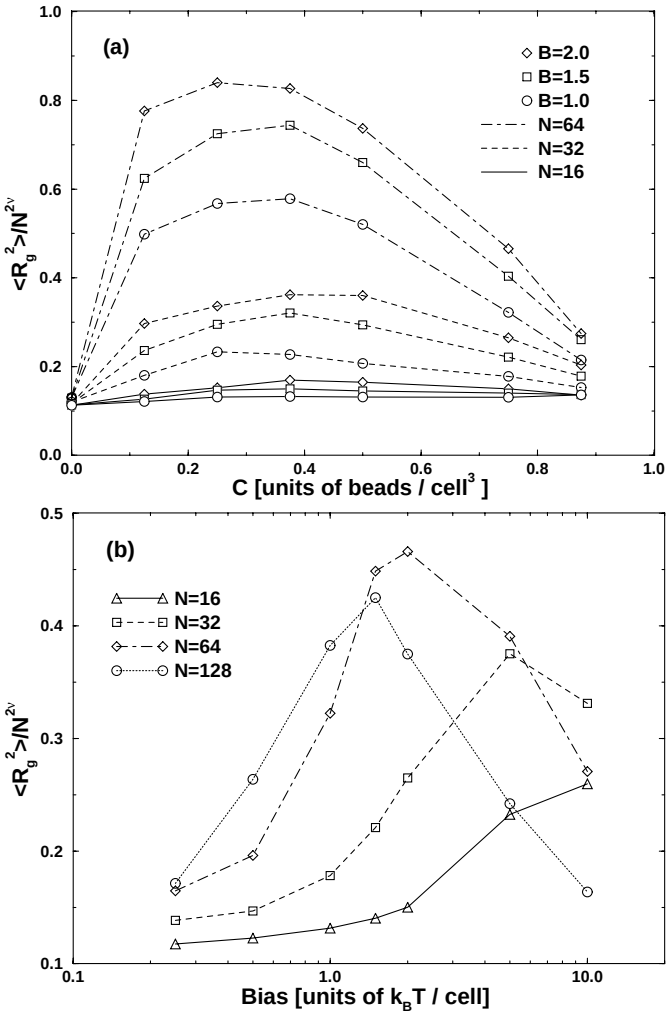

Fig. 6. (a) R_g scaled with $N^{2\nu}$ ($\nu = 0.59$) *vs.* C for chain lengths 16, 32 and 64 and *vs.* B (b) at $C = 0.75$ for $N = 16$, 32, 64 and 128.

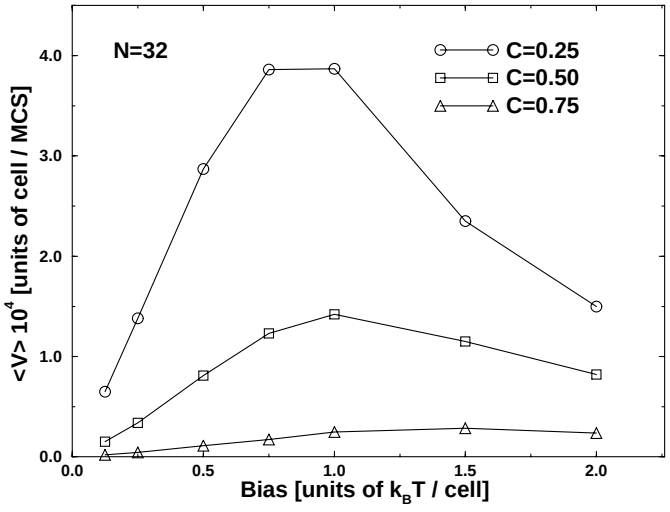

Fig. 7. Mean drift velocity *vs.* field, measured during 10^6 MCS of the simulations for chains with $N = 32$.

medium also experimentally. Theoretical work, considering flow of macromolecules through a random host matrix is also highly desirable. We hope that the present study will be helpful for such efforts.

A support from the NSF-EPSCoR grant is acknowledged. Simulations were performed at the Mississippi Center for Supercomputing Research, National University of Singapore and German Supercomputer Research Center HLRZ Jülich. A. Milchev and V. Yamakov acknowledge support from the Bulgarian Science Foundation under Grant No. X-644/1996.

References

1. K. Kremer, G.S. Grest, in *Monte Carlo and Molecular Dynamics Simulations in Polymer Science*, edited by K. Binder (Oxford University Press, New York, 1995), p. 194.
2. P.-G. de Gennes, *Scaling Concepts in Polymer Physics* (Cornell University Press, Ithaca, NY, 1979).
3. M. Doi, S.F. Edwards, *The Theory of Polymer Dynamics* (Clarendon Press, Oxford, 1986).
4. J. Bernasconi, W.R. Schneider, J. Phys. A **15**, L729 (1982).
5. R.B. Pandey, Phys. Rev. B **30**, 489 (1984).
6. E. Seifert, M. Suessenbach, J. Phys. A **17**, L703 (1984).
7. D. Stauffer, D. Sornette, Physica A **252**, 271 (1998); A. Kirsch, Int. J. Mod. Phys. **9**, No. 7 (1998); J. Draeger (private communication).
8. D. Sornette, Phys. Rep. **297**, 239 (1998).
9. V. Yamakov, D. Stauffer, A. Milchev, G. Foo, R. Pandey, Phys. Rev. Lett. **79**, 2356 (1997).
10. V. Yamakov, A. Milchev, Phys. Rev. E **55**, 1704 (1997).
11. V. Yamakov, A. Milchev, Phys. Rev. E **56**, 7043 (1997).
12. A. Ajdari, D. Mukamel, L. Peliti, J. Prost, J. Phys. I France **4**, 1551 (1994).
13. D. Long, J.L Viovy, A. Ajdari, Phys. Rev. Lett. **76**, 3858 (1996).
14. D. Long, J.L Viovy, A. Ajdari, J. Phys.-Cond. Matter **8**, 9471 (1996).
15. Z. Toroczkai, R.K.P. Zia, Phys. Lett. A **217**, 97 (1996).
16. G.M. Foo, R.B. Pandey, Phys. Rev. E. **51**, 5738 (1995).
17. G.M. Foo, R.B. Pandey, Physica A **241**, 500 (1997).
18. G.M. Foo, R.B. Pandey, Phys. Rev. E **55**, 4433 (1997).
19. G.M. Foo, R.B. Pandey, Macromol. Theory Simul. **7**, 283 (1998).
20. I. Gerroff, A. Milchev, W. Paul, K. Binder, J. Chem. Phys. **98**, 6526 (1993).
21. A. Milchev, W. Paul, K. Binder, J. Chem. Phys. **99**, 4786 (1993).
22. A. Milchev, K. Binder, Europhys. Lett. **26**, 671 (1994).
23. A. Milchev, W. Paul, K. Binder, Macromol. Theory Simul. **3**, 915 (1944).
24. A. Milchev, K. Binder, J. Phys. II France **6**, 21 (1995).
25. A. Milchev, K. Binder, Macromolec. **29**, 343 (1996).
26. A. Milchev, K. Binder, J. Comp.-Aided Des. **2**, 1 (1995).
27. S.B. Lee, S. Torquato, Phys. Rev. A **41**, 5338 (1990).
28. G.M. Foo, R.B. Pandey, D. Stauffer, Phys. Rev. E **53**, 5738 (1996).
29. H. Böttger, V.V. Bryskin, Phys. Stat. Sol. B **113**, 9 (1982).
30. M. Barma, D. Dhar, J. Phys. C **16**, 1451 (1983).